doi:10.1093/brain/awx344 BRAIN 2017: Page 1 of 10 | 1

BRAIN
A JOURNAL OF NEUROLOGY

Reduced LRRK2 in association with retromer dysfunction in post-mortem brain tissue from *LRRK2* mutation carriers

Ye Zhao,[1,2,3] Gayathri Perera,[1,3] Junko Takahashi-Fujigasaki,[4] Deborah C. Mash,[5] Jean Paul G. Vonsattel,[6] Akiko Uchino,[4] Kazuko Hasegawa,[7] R. Jeremy Nichols,[8] Janice L. Holton,[9] Shigeo Murayama,[4] Nicolas Dzamko[1,2,3] and Glenda M. Halliday[1,2,3]

Missense mutations in leucine-rich repeat kinase 2 (*LRRK2*) are pathogenic for familial Parkinson's disease. However, it is unknown whether levels of LRRK2 protein in the brain are altered in patients with LRRK2-associated Parkinson's disease. Because LRRK2 mutations are relatively rare, accounting for approximately 1% of all Parkinson's disease, we accessioned cases from five international brain banks to investigate levels of the LRRK2 protein, and other genetically associated Parkinson's disease proteins. Brain tissue was obtained from 17 *LRRK2* mutation carriers (12 with the G2019S mutation and five with the I2020T mutation) and assayed by immunoblot. Compared to matched controls and idiopathic Parkinson's disease cases, we found levels of LRRK2 protein were reduced in the LRRK2 mutation cases. We also measured a decrease in two other proteins genetically implicated in Parkinson's disease, the core retromer component, vacuolar protein sorting associated protein 35 (VPS35), and the lysosomal hydrolase, glucocerebrosidase (GBA). Moreover, the classical retromer cargo protein, cation-independent mannose-6-phosphate receptor (MPR300, encoded by *IGF2R*), was also reduced in the LRRK2 mutation cohort and protein levels of the receptor were correlated to levels of LRRK2. These results provide new data on LRRK2 protein expression in brain tissue from *LRRK2* mutation carriers and support a relationship between LRRK2 and retromer dysfunction in LRRK2-associated Parkinson's disease brain.

1 Brain and Mind Centre, Sydney Medical School, University of Sydney, Camperdown, 2050, Australia
2 School of Medical Sciences, University of NSW, Kensington, 2033, Australia
3 Neuroscience Research Australia, Randwick, 2031, Australia
4 Department of Neuropathology, Brain Bank for Aging Research, Tokyo Metropolitan Geriatric0 Hospital and Institute of Gerontology, Tokyo, 173-0015, Japan
5 University of Miami Brain Endowment Bank™, University of Miami Miller School of Medicine, Miami, Florida, 33136, USA
6 New York Brain Bank, Taub Institute for Research on Alzheimer's Disease and the Aging Brain, Columbia University, New York, 10032, USA
7 Department of Neurology, Sagamihara National Hospital, Kangawa, 252-0315, Japan
8 Parkinson's Institute and Clinical Center, Sunnyvale, California, 94085, USA
9 Queen Square Brain Bank, UCL Institute of Neurology, University College London, London, WC1N 1PJ, UK

Correspondence to: Nicolas Dzamko,
Brain and Mind Centre, University of Sydney, Camperdown, NSW, 2050, Australia
E-mail: nicolas.dzamko@sydney.edu.au

Correspondence may also be addressed to: Glenda Halliday,
Brain and Mind Centre, University of Sydney, Camperdown, NSW, 2050, Australia
E-mail: glenda.halliday@sydney.edu.au

Keywords: LRRK2; retromer; alpha-synuclein; kinase inhibitor; Parkinson's disease

Received July 3, 2017. Revised October 3, 2017. Accepted October 25, 2017.

Introduction

The leucine-rich repeat kinase 2 (LRRK2) protein has emerged as an exciting potential target for the therapeutic treatment of Parkinson's disease. At least six missense mutations in the *LRRK2* gene have been identified that predispose to an increased risk of inherited Parkinson's disease (Cookson, 2010). When measured using either autophosphorylation of LRRK2 (Sheng *et al.*, 2012), or phosphorylation of downstream Rab protein substrates (Steger *et al.*, 2016), all pathogenic mutations increase the kinase activity of LRRK2, at least in animal and cell culture models. Consequently, there has been much investment in the development and characterization of small molecule inhibitors of LRRK2 activity, and some early studies in preclinical models are suggestive of a protective effect of such compounds (Atashrazm and Dzamko, 2016). Efforts to further develop and translate LRRK2 therapeutics are ongoing and an important translational step is to build an understanding of LRRK2 expression and function in pathologically relevant human biospecimens.

We have previously comprehensively measured LRRK2 levels in post-mortem brain tissue from cases with idiopathic Parkinson's disease, and preclinical cases with Lewy body pathology restricted to the olfactory bulb, sympathetic ganglia, medulla oblongata, and/or locus coeruleus (Dzamko *et al.*, 2017). Compared to controls, we found an early upregulation of LRRK2 protein in the cases with restricted Lewy bodies, that was followed by a disease duration-dependent decrease in LRRK2 levels back to the same level as controls. However, little is known about LRRK2 expression in cases with *LRRK2* mutations for at least two reasons. The first is that characterized post-mortem mutation cases are very rare, and second, there has been much difficulty in ascertaining antibodies suitable for measuring LRRK2 in formalin-fixed brain tissue (Davies *et al.*, 2013; Dzamko *et al.*, 2017). In the current study we have obtained 17 LRRK2 mutation cases and compared levels of LRRK2 to idiopathic Parkinson's disease and also controls by immunoblot using our established methods. Twelve of the LRRK2 mutation cases contained the G2019S mutation, the most common *LRRK2* mutation that may account for up to 1% of all Parkinson's disease (Healy *et al.*, 2008). The remaining five cases contained the neighbouring I2020T mutation, found in the Sagamihara region in Japan (Hasegawa *et al.*, 2009). The cases were as expected for these two mutations (Kalia *et al.*, 2015), with the G2019S cases with Parkinson's disease having Lewy pathology and non-motor features by end-stage, while those Parkinson's disease cases with the I2020T mutation were without non-motor features and Lewy bodies.

Although *LRRK2* mutations confer enhanced risk of developing Parkinson's disease, it is generally regarded that these mutations are not fully penetrant, and thus other genetic and/or environmental factors likely contribute to disease conversion (Trinh *et al.*, 2014; Marder *et al.*, 2015). Thus, we measured the levels of LRRK2, and two other key proteins that are genetically implicated in Parkinson's disease, vacuolar protein sorting associated protein 35 (VPS35) and glucocerebrosidase (GBA), to determine whether these proteins were dysregulated in the LRRK2 mutation cases. VPS35 is a component of the retromer complex, which is involved in retrograde endosomal to trans-Golgi trafficking (Trousdale and Kim, 2015). Like LRRK2, missense mutations in *VPS35* are associated with dominantly inherited Parkinson's disease (Zimprich *et al.*, 2011; Struhal *et al.*, 2014), and studies in *Drosophila* have functionally linked LRRK2 and VPS35 in the same trafficking pathways that may mediate neurodegeneration (MacLeod *et al.*, 2013). GBA is a lysosomal glucosidase and heterozygous missense mutations in *GBA* are another genetic risk factor for Parkinson's disease (Brockmann and Berg, 2014). Both GBA and LRRK2 have been implicated in dysfunction of the lysosomal-autophagy pathway in Parkinson's disease (Gan-Or *et al.*, 2015), but it is unknown if either the GBA or VPS35 proteins are altered in brain tissue from *LRRK2* mutation carriers with Parkinson's disease.

Materials and methods

Cases

This study was approved by the University of NSW Human Research Ethics Advisory (#HC14046) and frozen brain tissue obtained from institutionally approved autopsy collections held by the Sydney Brain Bank, the Tokyo Metropolitan Brain Bank for Aging Research, the Queen Square Brain Bank for Neurological Disorders, the University of Miami Brain Endowment Bank and the New York Brain Bank at Columbia University. Demographic information is provided in Table 1. LRRK2 mutation cases were sourced worldwide and matched for age, gender and post-mortem delay to idiopathic Parkinson's disease cases, defined according to Dickson *et al.* (2009), and to unaffected control cases. The selection of controls was based on no recorded clinical diagnosis of neurological or psychiatric symptoms, and the absence of CNS pathology at autopsy, including Lewy bodies, neurofibrillary tangles or neuritic plaque pathology. The 17 LRRK2 mutation cases consisted of 12 with the G2019S mutation, and five with the neighbouring I2020T mutation. All LRRK2 and idiopathic Parkinson's disease cases had diagnosed levodopa-responsive Parkinson's disease, and all had loss of pigmented neurons in the substantia nigra at autopsy. Early-onset Parkinson's disease (younger than 50 years) was excluded. Except for Lewy pathology, described below, the changes in protein levels were consistent for both LRRK2 mutations and were combined for analysis as a single LRRK2 mutation group.

Protein extraction from brain tissue

Proteins were sequentially extracted from 100 mg of fresh-frozen brain tissue based on their solubility in Tris-buffered saline (TBS) and then sodium dodecyl sulphate (SDS) as described previously

Table 1 Demographic details

	Control	Idiopathic	LRRK2 Parkinson's disease		
			Combined	G2019S	I2020T
Sample size	14	13	17	12	5
Age at death, years	76 ± 1.9 (63–89)	79 ± 1.2 (72–85)	76 ± 1.8 (58–85)	78 ± 1.7 (65–85)	73 ± 4.3 (58–81)
Gender (male/female)	8/6	8/5	6/11	4/8	2/3
Braak Lewy stage, /6	NA	5 ± 0.2 (4.0–6.0)	3 ± 0.5 (0.0–6.0)	5 ± 0.2 (4.0–6.0)	0 ± 0.2(0.0–1.0)
Symptom duration, years	NA	15.62 ± 1.33 (10.0–26.0)	18.54 ± 2.39 (4.0–32.0)	17.00 ± 3.28 (4.0–32.0)	21.00 ± 3.45 (13.0–32.0)
Post-mortem delay, h	10.36 ± 1.81 (2.0–23.0)	14.62 ± 2.57 (5.0–32.0)	14.41 ± 3.06 (2.0–45.0)	16.67 ± 3.91 (4.0–45.0)	9.00 ± 3.95 (2.0–24.0)
Storage time, years	9.93 ± 0.85 (5.0–14.0)	5.46 ± 0.54* (3.0–9.0)	12.88 ± 1.59 (1.0–24.0)	13.83 ± 1.68 (1.0–24.0)	10.60 ± 3.71 (1.0–21.0)

Demographic data for the brain tissue cases used in this study are shown. Data are mean ± SEM with the range shown parentheses. The LRRK2 G2019S and I2020T mutation groups were combined into a single group for analysis. Demographic data for the individual mutation groups is shown for information. One-way ANOVA with the Tukey *post hoc* test was used to measure differences across the three groups (control, idiopathic Parkinson's disease and combined LRRK2 mutation Parkinson's disease). *$P < 0.05$ compared to both control and G2019S groups. NA = not applicable.

(Dzamko *et al.*, 2017). This protein extraction method is commonly used to monitor the solubility change that occurs for α-synuclein in Parkinson's disease and allows for protein levels to be examined in the context of α-synuclein pathology (Zhou *et al.*, 2011). The disease affected superior/middle frontal cortex, which has Lewy pathology without neuronal loss late in Parkinson's disease, and the disease unaffected occipital cortex, which is without neuronal loss or Lewy pathology in Parkinson's disease, were used for this study. Frozen substantia nigra, which has a substantial loss of neurons at end-stage Parkinson's disease, was not available for the LRRK2 mutation cases.

Protein quantitation and immunoblotting

The protein concentration of extracted lysates was determined by bicinchoninic acid assay (Pierce) and made up to 1 mg/ml in 1 × lithium dodecyl sulphate sample buffer (Thermo Fisher). Lysates were then separated on Novex 4-12% Tris Glycine SDS-PAGE gels (Thermo Fisher), except for ATP13A2, which was separated on 8% gels, and proteins transferred to nitrocellulose. Details of antibodies used for immunodetection are provided in Supplementary Table 1. For all antibodies, except Ser129 phosphorylated α-synuclein, membranes were blocked with 5% skimmed milk in TBS buffer containing 0.1% Tween-20 (Sigma), and incubated overnight as described previously (Dzamko *et al.*, 2017). For immunodetection of Ser129 phosphorylated α-synuclein, membranes were fixed with 4% paraformaldehyde and 0.1% glutaraldehyde (both from Sigma) prior to blocking and antibody incubation as above (Sasaki *et al.*, 2015). Images were captured using a ChemiDoc™ MP imaging system using either horseradish peroxidase-conjugated secondary antibodies in conjunction with enhanced chemiluminescence reagent (GE Healthcare), or Alexa Fluor® labelled secondary antibodies (Bio-Rad). The intensity of each protein band was then quantified and expressed as arbitrary units normalized to β-actin protein levels. Representative cropped immunoblots are included in the figures with example full-length immunoblots shown as Supplementary Fig. 1.

Statistics

All statistical analyses were performed using SPSS Statistics software (IBM, Chicago, IL), with statistical significance set at $P < 0.05$. One-way ANOVA with Tukey *post hoc* test was used to compare the demographic data across the groups, and confirmed no significant differences in age or post-mortem delay between groups. However, as we previously identified a significant relationship between LRRK2 protein levels and post-mortem delay (Dzamko *et al.*, 2017), post-mortem delay was covaried for in all uni- or multivariate analyses used to determine differences in protein levels between groups. Spearman correlations were performed to identify significant associations between different proteins, α-synuclein pathology or demographic variables.

Results

Reduced LRRK2 protein and phosphorylation in LRRK2 mutation cases

The protein levels of LRRK2 and the phosphorylation of LRRK2 at Ser910, Ser935 and Ser973 were first examined in the disease affected frontal cortex and compared across the three groups. Consistent with our previous report (Dzamko *et al.*, 2017), LRRK2 was only found in the SDS fraction and thus only this fraction was analysed. Multivariate analysis revealed a significant decrease (40%, $P < 0.05$) in the levels of LRRK2 in the frontal cortex of the LRRK2 mutation group compared to controls, whereas the idiopathic Parkinson's disease group was not significantly different from controls (Fig. 1A). After correction to total levels of LRRK2, there was a 29%, 23% and 33% decrease in LRRK2 Ser910, Ser935 and Ser973 phosphorylation in the LRRK2 mutation cases compared to controls (Fig. 1B–D). There was also a trend for reduced Ser935 phosphorylation in the idiopathic Parkinson's disease cases, whereas the other phosphorylation sites were not different from controls. Post-mortem delay, which was included as a covariate in the analyses, had no significant effect ($P = 0.139$). In the frontal cortex, no significant correlations were found between LRRK2 or measured demographic variables (Supplementary Table 2), although the levels of LRRK2 phosphorylation at Ser935 significantly declined

with increasing symptom duration (rho = −0.400, $P < 0.05$, Supplementary Table 2). We also examined levels of LRRK2 in the disease-unaffected occipital cortex, which as expected, was largely devoid of Ser129 phosphorylated α-synuclein (Supplementary Fig. 2). In the unaffected occipital cortex, levels of LRRK2 were even more markedly reduced (~60% decrease, $P < 0.001$) compared to both the idiopathic Parkinson's disease and control groups (Fig. 1E). After correction to levels of total LRRK2, there was a trend for reduced Ser910 and Ser935 phosphorylation in the occipital cortex, however this did not reach statistical significance (Supplementary Fig. 3). Again, post-mortem delay ($P = 0.623$) was used as a covariate in the multivariate analysis. In the occipital cortex there was an association between increased storage time and decreased LRRK2 levels (rho = −0.336, $P < 0.05$, Supplementary Table 2).

α-Synuclein pathology in LRRK2 mutation cases

In contrast to LRRK2, SDS-soluble α-synuclein phosphorylated at the pathological Ser129 residue was markedly increased in idiopathic Parkinson's disease frontal cortex (5-fold increase, $P < 0.01$) compared to controls. However, there was no significant increase in α-synuclein Ser129 phosphorylation in the frontal cortex of the LRRK2 mutation cases (Fig. 1F), despite similar symptom duration. This is likely due to known differences in α-synuclein deposition in the brains of subjects with different LRRK2 mutations (Kalia *et al.*, 2015), and indeed this was confirmed when the immunoblot analysis of phosphorylated α-synuclein was correlated with the immunohistochemical analysis of α-synuclein pathology based on Braak staging (rho = 0.434, $P < 0.05$, Supplementary Fig. 4). When the mutation group was considered as a whole, Braak Lewy stage was significantly reduced in the LRRK2 mutation cases (Table 1); however, this was substantially driven by the LRRK2 I2020T cases, in which Lewy bodies were not detected. When the LRRK2 I2020T cases were excluded and only the LRRK2 G2019S cases considered, the Braak Lewy stage was similar between LRRK2 mutation and idiopathic Parkinson's disease cases (Table 1). Levels of Ser129 phosphorylated α-synuclein did not correlate with levels of LRRK2 or LRRK2 phosphorylation in the cohorts (Supplementary Table 2).

Reduced soluble GBA in idiopathic Parkinson's disease and LRRK2 mutation cases

As LRRK2 has been implicated in lysosomal function, we investigated if Parkinson's disease implicated lysosomal proteins were altered in the LRRK2-mutation cases. In particular, we measured levels of GBA, along with levels of the cation transporting ATPase 13A2 (ATP13A2), cathepsin D (CatD) and lysosome-associated membrane protein 2A (LAMP2A). For both idiopathic Parkinson's disease and the LRRK2 mutation cases, GBA was decreased in the TBS fraction by 24% and 52%, respectively in the affected frontal cortex, whereas in the SDS fraction it was not significantly different (Fig. 2A and B). Levels of GBA did not associate with levels of LRRK2, Braak Lewy stage or storage time; however, there was a significant correlation of TBS-soluble GBA with symptom duration (Supplementary Table 3). LAMP2A and ATP13A2 were present in the SDS-soluble fraction and a non-significant trend for decreased LAMP2A of ~20% was observed in the frontal cortex for both idiopathic Parkinson's disease and the LRRK2 mutation cases compared to controls (Fig. 2C). There were no significant differences between the groups for levels of ATP13A2 in the frontal cortex (Supplementary Fig. 5). CatD was present in both the TBS and SDS soluble fractions but was not significantly different across the three groups (Supplementary Fig. 5). Post-mortem delay was included as a covariate in all analysis, but only for CatD did post-mortem delay have a significant effect on protein levels ($P < 0.01$). The TBS-soluble fraction of CatD, but not the other lysosomal proteins (Supplementary Table 3), was also negatively correlated with storage time (rho = −0.542, $P < 0.001$), indicating decreasing levels of TBS CatD with increased storage (Supplementary Fig. 6). Levels of TBS CatD, however, did correlate with levels of phosphorylated α-synuclein (rho = 0.387, $P < 0.01$, Fig. 2D), while LAMP2A (rho = 0.304, $P < 0.05$, Fig. 2E) and ATP13A2 (rho = 0.331, $P < 0.05$, Fig. 2F) correlated with levels of LRRK2 in the frontal cortex (Supplementary Table 3). In the unaffected occipital cortex there was no change in the levels of TBS soluble GBA (Fig. 2G); however, LAMP2A was significantly reduced in the LRRK2 mutation cases (Fig. 2H). The levels of LAMP2A did not correlate with LRRK2 in this brain region.

Reduced Tris-buffered saline-soluble VPS35 and reduced MPR300 in LRRK2 mutation cases

LRRK2 has been linked to retromer function so we also investigated levels of the key retromer proteins VPS35, and the cation-independent mannose-6-phosphate receptor (MPR300, encoded by *IGF2R*). Similar to GBA, levels of TBS-soluble VPS35 were decreased in both idiopathic Parkinson's disease and the LRRK2 mutation cases in the affected frontal cortex, by 32% and 50%, respectively, whereas in the SDS fraction VPS35 levels were not significantly different (Fig. 3A and B). Post-mortem delay was included as a covariate in the analysis but had no significant effect ($P = 0.290$). There was no association of VPS35 with storage time, LRRK2 levels or Braak Lewy stage (Supplementary Table 4); however, there was a significant negative correlation between TBS and SDS-soluble VPS35

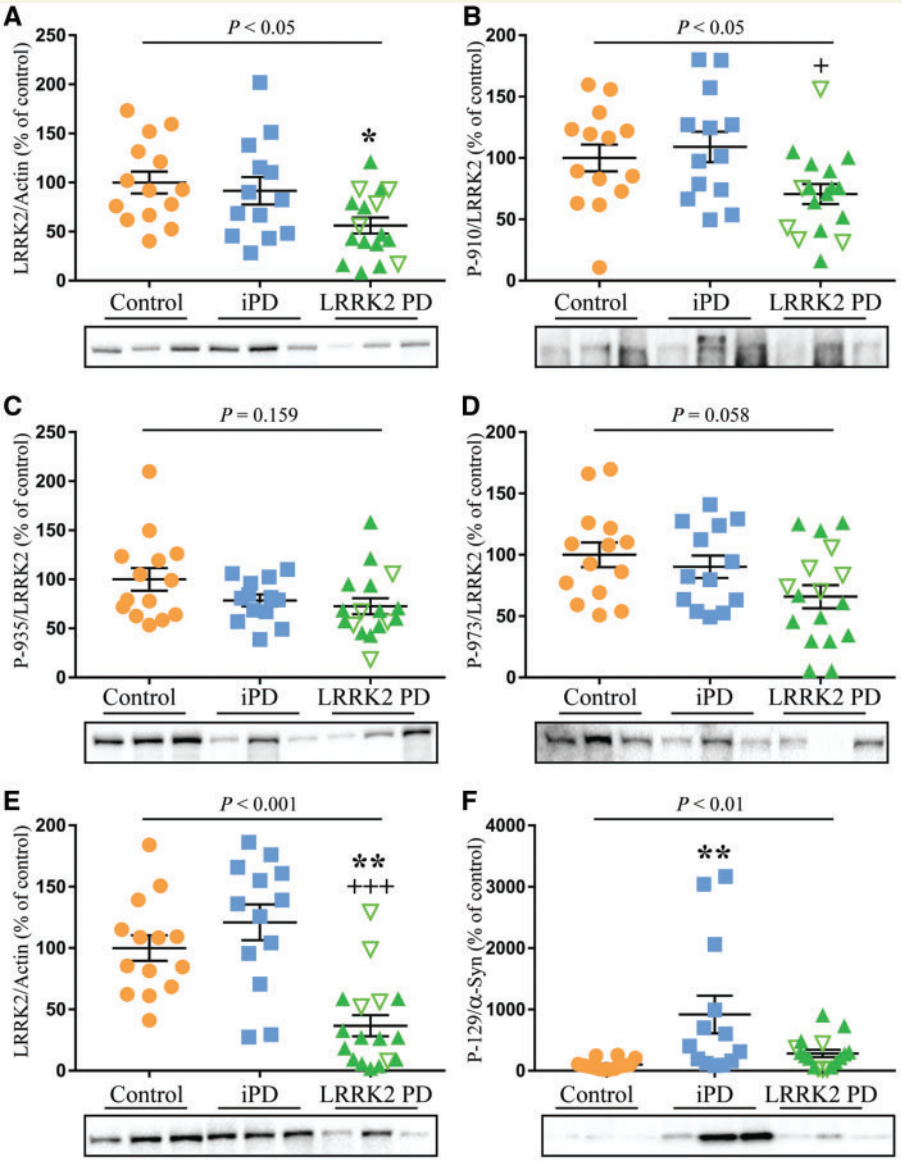

Figure 1 Reduced LRRK2 levels in post-mortem brain with LRRK2 mutations. Multivariate analysis covarying for post-mortem delay was used to assess changes in protein levels of leucine-rich repeat kinase 2 (LRRK2) in the frontal cortex (**A**), as well as the levels of LRRK2 phosphorylation on Ser910, Ser935 and Ser973 in frontal cortex (**B–D**) and levels of LRRK2 in occipital cortex (**E**) of controls (n = 14), idiopathic Parkinson's disease (iPD, n = 13) and LRRK2-associated Parkinson's disease cases (n = 17). Levels of α-synuclein phosphorylated at Ser129 were also measured in the frontal cortex (**F**). The LRRK2 mutation cohort consisted of cases with the G2019S mutation (green filled triangles) and the I2020T mutation (upturned green unfilled triangles). P-values indicate whether or not there was a significant effect of Parkinson's disease in the multivariate analysis. Subsequent *post hoc* analysis was used to identify significantly different groups with $^{*}P < 0.05$ and $^{**}P < 0.01$ compared to controls and $^{+}P < 0.05$ and $^{+++}P < 0.001$ compared to the idiopathic Parkinson's disease group. Individual data points are shown on the graph as well as mean ± standard error of the mean (SEM). Representative immunoblots are shown with uncropped examples available in the Supplementary material. LRRK2 immunoblots were normalized to β-actin and values expressed as the per cent of control cases, which were set at 100%. Phosphorylated proteins were corrected to the levels of the corresponding total protein.

(rho = −0.328, $P < 0.05$, Fig. 3C), indicating a change in solubility. In the unaffected occipital cortex, the TBS fraction of VPS35 was again significantly reduced in both Parkinson's disease groups (Fig. 3D). Levels of MPR300, which were detected only in the SDS fraction, showed a 38% decrease in the frontal cortex in the mutation cases compared to controls and a significant 77% reduction compared to the idiopathic Parkinson's disease group ($P < 0.05$, Fig. 3E). Post-mortem delay, which was included as a covariate in the univariate analysis, again had no significant effect ($P = 0.188$). There was no association between MPR300 levels and storage time (Supplementary Table 4); however, there was a significant correlation between levels of MPR300 and LRRK2 (rho = 0.392, $P < 0.01$, Fig. 3F). MPR300 was also reduced in the occipital cortex of the mutation cases

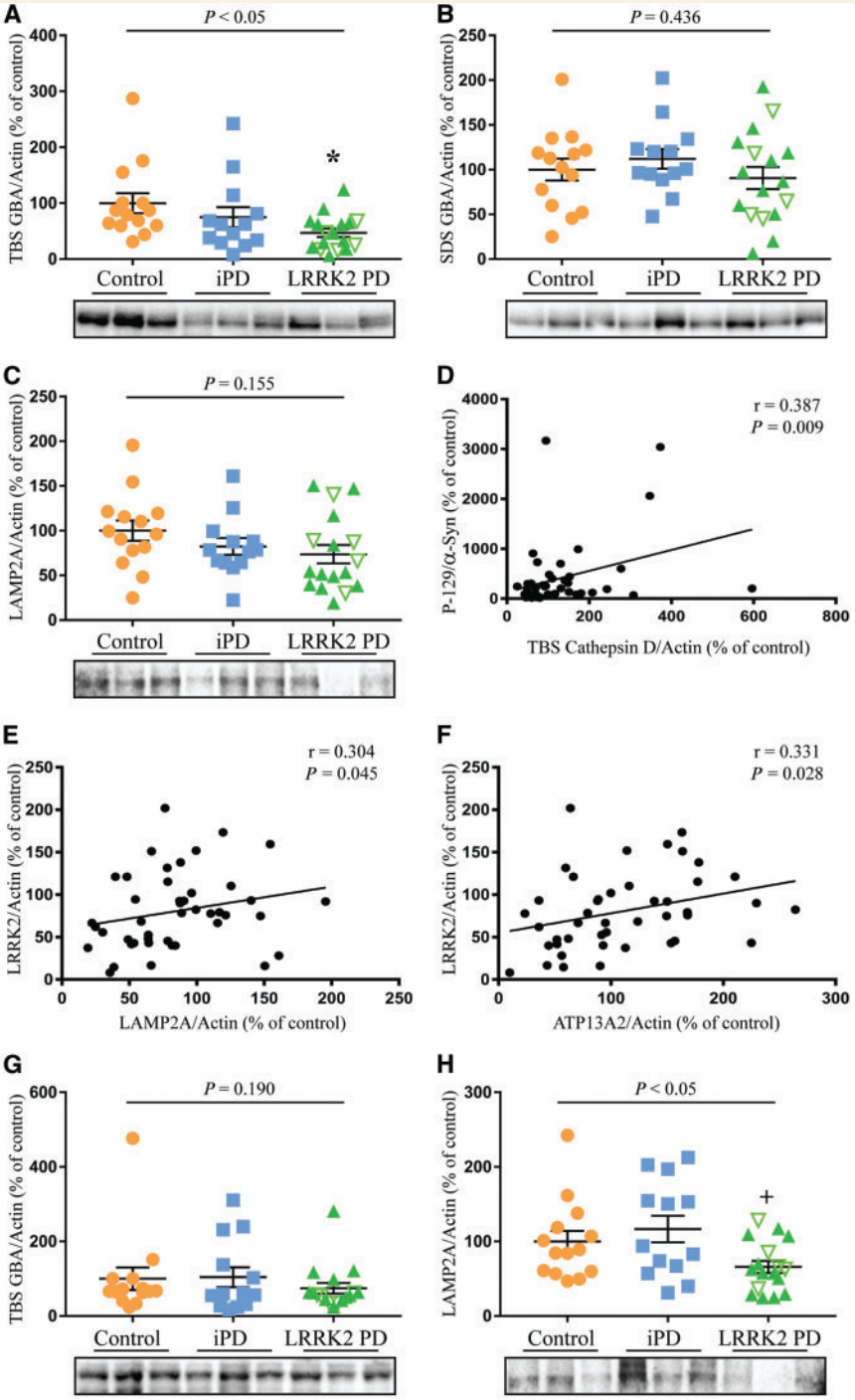

Figure 2 Reduced TBS-soluble GBA levels in post-mortem brain with LRRK2 mutations. Multivariate analysis covarying for post-mortem delay was used to assess changes in protein levels of GBA, ATP13A2, cathepsin D (CatD) and lysosome-associated membrane protein 2A (LAMP2A) in controls (n = 14), idiopathic Parkinson's disease (iPD, n = 13) and LRRK2-associated Parkinson's disease cases (n = 17). (**A** and **B**) TBS and SDS soluble levels of GBA in the frontal cortex. (**C**) Levels of LAMP2A in the frontal cortex. (**D**) Spearman analysis revealed a significant correlation between levels of phosphorylated α-synuclein and TBS-soluble CatD, as well as significant correlations between LRRK2 and LAMP2A (**E**), and LRRK2 and ATP13A2 (**F**). (**G**) Levels of TBS soluble GBA in the occipital cortex. (**H**) Levels of LAMP2A in the occipital cortex. The LRRK2 mutation cohort consisted of cases with the G2019S mutation (green filled triangles) and the I2020T mutation (upturned green unfilled triangles). *P*-values indicate a significant effect of Parkinson's disease in the multivariate analysis. Subsequent *post hoc* analysis was used to identify significantly different groups with $^{*}P < 0.05$ compared to controls and $^{+}P < 0.05$ compared to the idiopathic Parkinson's disease cases. Individual data points are shown on the graph as well as mean ± SEM. Representative immunoblots are shown with uncropped examples available in the Supplementary material. Immunoblots were normalized to β-actin and values expressed as the per cent of control cases, which were set at 100%.

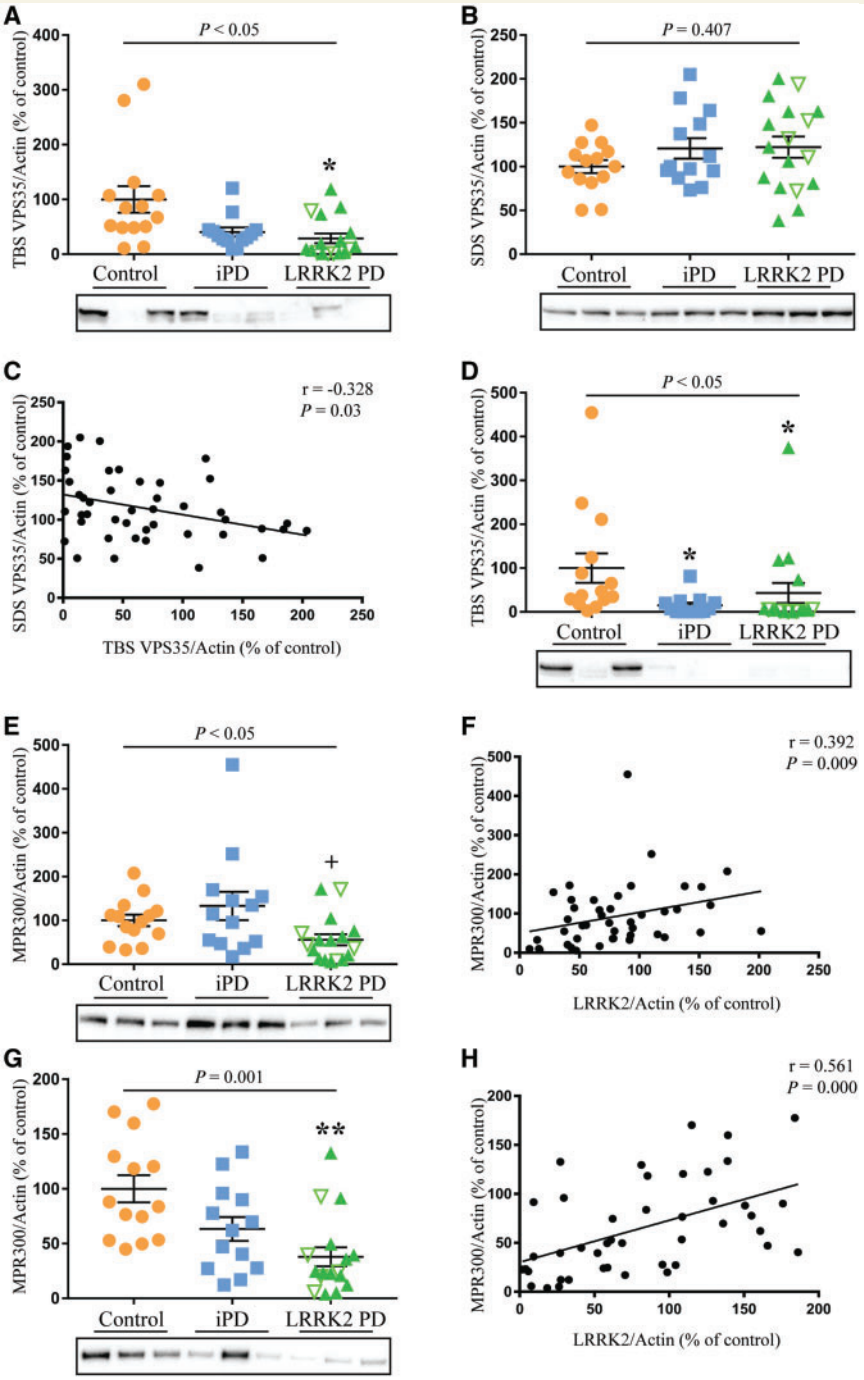

Figure 3 Reduced TBS-soluble VPS35 and reduced MPR300 in LRRK2 mutation cases. Multivariate analysis covarying for post-mortem delay was used to assess changes in protein levels of VPS35 and MPR300 in controls (n = 14), idiopathic Parkinson's disease (iPD, n = 13) and LRRK2-associated Parkinson's disease cases (n = 17). (**A** and **B**) Levels of TBS and SDS soluble VPS35 in the frontal cortex. (**C**) Spearman analysis revealed a significant negative correlation between the levels of TBS- and SDS-soluble VPS35. (**D**) Levels of TBS-soluble VPS35 in the occipital cortex. (**E**) Levels of MPR300 in the frontal cortex. (**F**) Spearman analysis revealed a significant correlation between the levels of MPR300 and LRRK2 in the frontal cortex. (**G**) Levels of MPR300 in the occipital cortex. (**H**) Spearman analysis revealed a significant correlation between the levels of MPR300 and LRRK2 in the occipital cortex. The LRRK2 mutation cohort consisted of cases with the G2019S mutation (green filled triangles) and the I2020T mutation (upturned green unfilled triangles). P-values indicate a significant effect of Parkinson's disease in the univariate analysis. Subsequent *post hoc* analysis was used to identify significantly different groups with $^{*}P < 0.05$, $^{**}P < 0.01$ compared to controls and $^{+}P < 0.05$ compared to the idiopathic Parkinson's disease cases. Individual data points are shown on the graph as well as mean ± SEM. Representative immunoblots are shown with uncropped examples available in the Supplementary material. Immunoblots were normalized to β-actin and values expressed as the per cent of control cases, which were set at 100%.

compared to the control group (~60%, $P < 0.01$, Fig. 3G) and was again significantly associated with levels of LRRK2 (rho = 0.561, $P < 0.001$, Fig. 3H).

Discussion

Missense mutations in *LRRK2* predispose to Parkinson's disease. In particular, pathogenic *LRRK2* mutations increase the enzymes kinase activity and there is accumulating evidence that the increased kinase activity mediates LRRK2 pathobiology. Moreover, potent and selective inhibitors of LRRK2 kinase activity are in advanced stages of development. There is now much interest in determining whether such compounds could be used therapeutically for *LRRK2* mutation carriers. An important part of this process is to understand levels of LRRK2 in human biospecimens. Characterized post-mortem brain tissue from symptomatic *LRRK2* mutation carriers is extremely rare. Our study investigates 17 Parkinson's disease cases with *LRRK2* mutations, which to the best of our knowledge is the majority of known and characterized cases worldwide, with available frozen tissue samples. The LRRK2 mutation cases had typical features, particularly the lack of Lewy pathology in I2020T cases (Kalia *et al.*, 2015). We have used immunoblotting to measure LRRK2 and other Parkinson's disease-implicated proteins in cortical brain tissue from these *LRRK2* mutation carriers, and have compared the protein levels to both idiopathic Parkinson's disease cases and neurologically normal controls.

Previously, we have mapped the expression of LRRK2 protein in post-mortem idiopathic Parkinson's disease brain and in preclinical Parkinson's disease cases with restricted Lewy bodies (Dzamko *et al.*, 2017). We showed that LRRK2 protein was increased in the preclinical cases, and then it decreased back to the same levels as controls in a symptom duration-dependent manner. In the current study, levels of LRRK2 were again similar between control and idiopathic Parkinson's disease, however, the levels were reduced in the Parkinson's disease cases with *LRRK2* mutations. Reduced LRRK2 was found in both the frontal and occipital cortex and was not associated with Lewy pathology. This suggests that reduced LRRK2 is either a result of the pathogenic mutations, or potential caveats associated with post-mortem brain studies. In regard to the latter, cases were matched for age, gender and post-mortem delay. All Parkinson's disease cases also had similar symptom durations. However, the idiopathic Parkinson's disease cases had been in freezer storage for less time compared to the control and LRRK2 mutation cases. Longer storage time was associated with lower LRRK2 levels, at least in the occipital cortex. As the storage time was similar between control and LRRK2 mutation cases, it seems unlikely that this variable would completely explain the decreased LRRK2 levels in the mutation cases, albeit, increased storage time may have intensified the magnitude of the results. We would recommend to others using these rare LRRK2 mutation tissue samples to consider the freezer storage time when matching affected and control groups.

Reduced endogenous LRRK2 levels in association with pathogenic *LRRK2* mutations has not been routinely observed. A number of studies have investigated the expression of LRRK2 in primary human fibroblasts from Parkinson's disease cases and controls, and reported similar levels of LRRK2 protein, albeit with very small sample sizes and a diverse selection of antibodies (Devine *et al.*, 2011; Papkovskaia *et al.*, 2012; Garcia-Miralles *et al.*, 2015; Smith *et al.*, 2016). LRRK2 G2019S knock-in mice also have similar levels of LRRK2 protein (Garcia-Miralles *et al.*, 2015). Difficulty in detecting LRRK2, particularly in fixed brain tissues has, however, made an assessment of LRRK2 levels in post-mortem brain and human neural cell cultures challenging. One study has reported a trend for decreased *LRRK2* mRNA in the cortex of LRRK2 G2019S brain tissue (Sharma *et al.*, 2011) and these cases are also included in the current study. It is also reported that LRRK2 inhibitors can destabilize LRRK2 and reduce protein levels (Lobbestael *et al.*, 2016), suggesting a dynamic interaction between LRRK2 enzyme activity and its protein levels. If LRRK2 protein is reduced in the brain of pathogenic *LRRK2* mutation carriers, this would reduce the pool of LRRK2 that can be actively targeted with inhibitor therapy, especially with advancing disease progression at end-stage disease. It may be important to determine if *LRRK2* mutation carriers have an earlier increase in LRRK2 protein levels, similar to the early increase reported for idiopathic Parkinson's disease brain (Dzamko *et al.*, 2017). Novel radioligands for LRRK2 may make such studies possible in the future (Malik *et al.*, 2017). Moreover, it will be important to determine the relationship between LRRK2 protein and LRRK2 kinase activity, studies that could potentially be achieved by measuring phosphorylation levels of recently described LRRK2 substrates, such as the Rab GTPases (Steger *et al.*, 2016), when suitable techniques become available.

As previously identified in idiopathic Parkinson's disease (Murphy *et al.*, 2014), there was a reduction in soluble GBA levels in Parkinson's disease cases with *LRRK2* mutations. GBA is a lysosomal enzyme required for glycolipid metabolism, with homozygous *GBA* mutations producing a lysosomal storage disorder while heterozygous *GBA* mutations are a risk factor for Parkinson's disease (Siebert *et al.*, 2014). Reduced GBA function is associated with elevated α-synuclein (Murphy *et al.*, 2014), but not all Parkinson's disease cases with LRRK2 mutations have elevated α-synuclein, for example the I2020T cases in the present study. This suggests an alternate mechanism for reduced GBA and LRRK2 is likely in these cases. In this regard, levels of LRRK2 in the frontal cortex did correlate with two other lysosomal proteins, LAMP2A and ATP13A2. In particular, LAMP2A has been reported to be decreased in Parkinson's disease

(Murphy *et al.*, 2015), including in cases with LRRK2 G2019S mutations (Henry *et al.*, 2015). Moreover, LAMP2A contributes to LRRK2 turnover through chaperone-mediated autophagy, although the G2019S mutation is thought to render LRRK2 a poorer substrate for degradation via this pathway (Orenstein *et al.*, 2013).

Like *LRRK2*, missense mutations in *VPS35* are pathogenic for autosomal dominant Parkinson's disease, which is largely indistinguishable from idiopathic Parkinson's disease (Vilarino-Guell *et al.*, 2011; Zimprich *et al.*, 2011; Struhal *et al.*, 2014; Williams *et al.*, 2017). In *Drosophila*, LRRK2 and VPS35 have been functionally linked and suggested to converge on the same biological pathway of intraneuronal lysosomal/Golgi sorting to mediate neurodegeneration (MacLeod *et al.*, 2013). Indeed, overexpression of VPS35 can rescue the neurodegenerative phenotype induced in *Drosophila* by either the LRRK2 G2019S mutation (MacLeod *et al.*, 2013) or the LRRK2 I2020T mutation (Linhart *et al.*, 2014), strongly suggesting an interplay between these two important Parkinson's disease proteins. Our new data further support this concept as we observed an apparent solubility shift in VPS35, with a reduction in TBS-soluble protein and an associated increase in the SDS-soluble VPS35, particularly in the *LRRK2* mutation cases. This change in solubility was independent of Lewy pathology. Such a shift could result from impaired localization and may be indicative of retromer or lysosomal dysfunction. VPS35 deficiency or mutation impairs endosomal to Golgi retrieval of LAMP2A, which could impact on the levels of LRRK2 as described above (Orenstein *et al.*, 2013). It should be noted that VPS35 levels have previously been reported to be similar to controls in both idiopathic Parkinson's disease and LRRK2 G2019S post-mortem brains (Tsika *et al.*, 2014). In this prior study, brain protein was extracted using only a single buffer, in contrast to our current study that performed the sequential TBS, SDS extraction commonly used to measure the accumulation of pathogenic α-synuclein in Parkinson's disease brain (Zhou *et al.*, 2011). Using this method, we observed reduced TBS-soluble VPS35 with increased SDS-soluble VPS35, consistent with the reported no net change in total VPS35 levels. This does, however, indicate a change in VPS35 associations likely to reflect retromer dysfunction. Indeed, the retromer cargo protein, MPR300, was reduced in the LRRK2 mutation cases, which can occur through increased lysosomal degradation or extracellular secretion when the protein is no longer trafficked properly (Matrone *et al.*, 2016). Moreover, reduced levels of MPR300 were associated with reduced levels of LRRK2. Therefore, it may be important to model and understand the dynamic relationship between LRRK2 and retromer, particularly in regard to whether retromer dysfunction contributes to the conversion of asymptomatic *LRRK2* mutation carriers to Parkinson's disease.

The study of these Parkinson's disease cases with LRRK2 mutation has provided important novel information. Despite differences in the dysregulation of α-synuclein between the G2019S versus the I2020T LRRK2 mutations, similar reductions in the levels of LRRK2, GBA and the retromer cargo protein MPR300 were observed, as well as a shift in the solubility of VPS35. The reductions in these measures were more marked in Parkinson's disease cases with *LRRK2* mutations compared to those observed in idiopathic Parkinson's disease, which had more marked increases in phosphorylated α-synuclein compared with the *LRRK2* mutation cases. The severity of these protein deficits were related to each other, suggesting the involvement of related intracellular pathways. These data suggest that *LRRK2* mutation carriers have more substantial retromer dysfunction compared with idiopathic Parkinson's disease, and that such dysfunction does not necessarily cause the aggregation of α-synuclein.

Acknowledgements

We thank the following brain banks for tissue used in this study: the Sydney Brain Bank Australia, the Tokyo Brain Bank for Aging Research, the Queens Square Brain Bank UK, the New York Brain Bank USA, and the University of Miami Brain Endowment Bank USA. We thank Shikara Keshiya for technical assistance.

Funding

This work was supported by a research grant jointly funded by the Michael J Fox Foundation for Parkinson's Disease Research and the Shake It Up Australia Foundation (awarded to G.M.H., N.D., S.M., R.J.N. and J.L.H.) and by a Parkinson's New South Wales seed grant awarded to ND. YZ holds a scholarship from the University of New South Wales and an Elizabeth-Gilbert Scholarship from Neuroscience Research Australia. G.M.H. holds a senior principal research fellowship from the National Health and Medical Research Council of Australia (#1079679). J.L.H. is supported by the Multiple System Atrophy Trust, Alzheimer's Research UK. Tissues received from the Sydney Brain Bank at Neuroscience Research Australia were collected with funding from the University of New South Wales and Neuroscience Research Australia. Queen Square Brain Bank is supported by Reta Lila Weston Institute for Neurological Studies and the Medical Research Council UK. The University of Miami Brain Endowment Bank USA is a National Institutes of Health funded NeuroBioBank funded by contract support provided by the National Institute of Neurological Disorders and Stroke, the National Institute of Mental Health and the National Institute of Child Health and Development. LRRK2 autopsy collection at Columbia University was funded by the Parkinson's Disease Foundation and the Michael J Fox Foundation.

Supplementary material

Supplementary material is available at *Brain* online.

References

Atashrazm F, Dzamko N. LRRK2 inhibitors and their potential in the treatment of Parkinson's disease: current perspectives. Clin Pharmacol 2016; 8: 177–89.

Brockmann K, Berg D. The significance of GBA for Parkinson's disease. J Inherit Metab Dis 2014; 37: 643–8.

Cookson MR. The role of leucine-rich repeat kinase 2 (LRRK2) in Parkinson's disease. Nat Rev Neurosci 2010; 11: 791–7.

Davies P, Hinkle KM, Sukar NN, Sepulveda B, Mesias R, Serrano G, et al. Comprehensive characterization and optimization of anti-LRRK2 (leucine-rich repeat kinase 2) monoclonal antibodies. Biochem J 2013; 453: 101–13.

Devine MJ, Kaganovich A, Ryten M, Mamais A, Trabzuni D, Manzoni C, et al. Pathogenic LRRK2 mutations do not alter gene expression in cell model systems or human brain tissue. PLoS One 2011; 6: e22489.

Dickson DW, Braak H, Duda JE, Duyckaerts C, Gasser T, Halliday GM, et al. Neuropathological assessment of Parkinson's disease: refining the diagnostic criteria. Lancet Neurol 2009; 8: 1150–7.

Dzamko N, Gysbers AM, Bandopadhyay R, Bolliger MF, Uchino A, Zhao Y, et al. LRRK2 levels and phosphorylation in Parkinson's disease brain and cases with restricted Lewy bodies. Mov Disord 2017; 32: 423–32.

Gan-Or Z, Dion PA, Rouleau GA. Genetic perspective on the role of the autophagy-lysosome pathway in Parkinson disease. Autophagy 2015; 11: 1443–57.

Garcia-Miralles M, Coomaraswamy J, Habig K, Herzig MC, Funk N, Gillardon F, et al. No dopamine cell loss or changes in cytoskeleton function in transgenic mice expressing physiological levels of wild type or G2019S mutant LRRK2 and in human fibroblasts. PLoS One 2015; 10: e0118947.

Hasegawa K, Stoessl AJ, Yokoyama T, Kowa H, Wszolek ZK, Yagishita S. Familial parkinsonism: study of original Sagamihara PARK8 (I2020T) kindred with variable clinicopathologic outcomes. Parkinsonism Relat Disord 2009; 15: 300–6.

Healy DG, Falchi M, O'Sullivan SS, Bonifati V, Durr A, Bressman S, et al. Phenotype, genotype, and worldwide genetic penetrance of LRRK2-associated Parkinson's disease: a case-control study. Lancet Neurol 2008; 7: 583–90.

Henry AG, Aghamohammadzadeh S, Samaroo H, Chen Y, Mou K, Needle E, et al. Pathogenic LRRK2 mutations, through increased kinase activity, produce enlarged lysosomes with reduced degradative capacity and increase ATP13A2 expression. Hum Mol Genet 2015; 24: 6013–28.

Kalia LV, Lang AE, Hazrati LN, Fujioka S, Wszolek ZK, Dickson DW, et al. Clinical correlations with Lewy body pathology in LRRK2-related Parkinson disease. JAMA Neurol 2015; 72: 100–5.

Linhart R, Wong SA, Cao J, Tran M, Huynh A, Ardrey C, et al. Vacuolar protein sorting 35 (Vps35) rescues locomotor deficits and shortened lifespan in Drosophila expressing a Parkinson's disease mutant of Leucine-Rich Repeat Kinase 2 (LRRK2). Mol Neurodegener 2014; 9: 23.

Lobbestael E, Civiero L, De Wit T, Taymans JM, Greggio E, Baekelandt V. Pharmacological LRRK2 kinase inhibition induces LRRK2 protein destabilization and proteasomal degradation. Sci Rep 2016; 6: 33897.

MacLeod DA, Rhinn H, Kuwahara T, Zolin A, Di Paolo G, McCabe BD, et al. RAB7L1 interacts with LRRK2 to modify intraneuronal protein sorting and Parkinson's disease risk. Neuron 2013; 77: 425–39.

Malik N, Gifford AN, Sandell J, Tuchman D, Ding YS. Synthesis and *in vitro* and *in vivo* evaluation of [3H]LRRK2-IN-1 as a novel radioligand for LRRK2. Mol Imaging Biol 2017; 19: 837–45.

Marder K, Wang Y, Alcalay RN, Mejia-Santana H, Tang MX, Lee A, et al. Age-specific penetrance of LRRK2 G2019S in the Michael J. Fox Ashkenazi Jewish LRRK2 Consortium. Neurology 2015; 85: 89–95.

Matrone C, Dzamko N, Madsen P, Nyegaard M, Pohlmann R, Sondergaard RV, et al. Mannose 6-phosphate receptor is reduced in α-synuclein overexpressing models of Parkinsons disease. PLoS One 2016; 11: e0160501.

Murphy KE, Gysbers AM, Abbott SK, Spiro AS, Furuta A, Cooper A, et al. Lysosomal-associated membrane protein 2 isoforms are differentially affected in early Parkinson's disease. Mov Disord 2015; 30: 1639–47.

Murphy KE, Gysbers AM, Abbott SK, Tayebi N, Kim WS, Sidransky E, et al. Reduced glucocerebrosidase is associated with increased alpha-synuclein in sporadic Parkinson's disease. Brain 2014; 137 (Pt 3): 834–48.

Orenstein SJ, Kuo SH, Tasset I, Arias E, Koga H, Fernandez-Carasa I, et al. Interplay of LRRK2 with chaperone-mediated autophagy. Nat Neurosci 2013; 16: 394–406.

Papkovskaia TD, Chau KY, Inesta-Vaquera F, Papkovsky DB, Healy DG, Nishio K, et al. G2019S leucine-rich repeat kinase 2 causes uncoupling protein-mediated mitochondrial depolarization. Hum Mol Genet 2012; 21: 4201–13.

Sasaki A, Arawaka S, Sato H, Kato T. Sensitive western blotting for detection of endogenous Ser129-phosphorylated alpha-synuclein in intracellular and extracellular spaces. Sci Rep 2015; 5: 14211.

Sharma S, Bandopadhyay R, Lashley T, Renton AE, Kingsbury AE, Kumaran R, et al. LRRK2 expression in idiopathic and G2019S positive Parkinson's disease subjects: a morphological and quantitative study. Neuropathol Appl Neurobiol 2011; 37: 777–90.

Sheng Z, Zhang S, Bustos D, Kleinheinz T, Le Pichon CE, Dominguez SL, et al. Ser1292 autophosphorylation is an indicator of LRRK2 kinase activity and contributes to the cellular effects of PD mutations. Sci Transl Med 2012; 4: 164ra1.

Siebert M, Sidransky E, Westbroek W. Glucocerebrosidase is shaking up the synucleinopathies. Brain 2014; 137 (Pt 5): 1304–22.

Smith GA, Jansson J, Rocha EM, Osborn T, Hallett PJ, Isacson O. Fibroblast biomarkers of sporadic Parkinson's disease and LRRK2 kinase inhibition. Mol Neurobiol 2016; 53: 5161–77.

Steger M, Tonelli F, Ito G, Davies P, Trost M, Vetter M, et al. Phosphoproteomics reveals that Parkinson's disease kinase LRRK2 regulates a subset of Rab GTPases. Elife 2016; 5: e12813. doi: 10.7554/eLife.12813.

Struhal W, Presslauer S, Spielberger S, Zimprich A, Auff E, Bruecke T, et al. VPS35 Parkinson's disease phenotype resembles the sporadic disease. J Neural Transm 2014; 121: 755–9.

Trinh J, Guella I, Farrer MJ. Disease penetrance of late-onset parkinsonism: a meta-analysis. JAMA Neurol 2014; 71: 1535–9.

Trousdale C, Kim K. Retromer: structure, function, and roles in mammalian disease. Eur J Cell Biol 2015; 94: 513–21.

Tsika E, Glauser L, Moser R, Fiser A, Daniel G, Sheerin UM, et al. Parkinson's disease-linked mutations in VPS35 induce dopaminergic neurodegeneration. Hum Mol Genet 2014; 23: 4621–38.

Vilarino-Guell C, Wider C, Ross OA, Dachsel JC, Kachergus JM, Lincoln SJ, et al. VPS35 mutations in Parkinson disease. Am J Hum Genet 2011; 89: 162–7.

Williams ET, Chen X, Moore DJ. VPS35, the retromer complex and Parkinson's disease. J Parkinsons Dis 2017; 7: 219–33.

Zhou J, Broe M, Huang Y, Anderson JP, Gai WP, Milward EA, et al. Changes in the solubility and phosphorylation of alpha-synuclein over the course of Parkinson's disease. Acta Neuropathol 2011; 121: 695–704.

Zimprich A, Benet-Pages A, Struhal W, Graf E, Eck SH, Offman MN, et al. A mutation in VPS35, encoding a subunit of the retromer complex, causes late-onset Parkinson disease. Am J Hum Genet 2011; 89: 168–75.